



# Mechanical and electrochemical characterization of Ti–12Mo–5Zr alloy for biomedical application

Changli Zhao<sup>a</sup>, Xiaonong Zhang<sup>a,\*</sup>, Peng Cao<sup>b</sup>

<sup>a</sup> State Key Laboratory of Metal Matrix Composites, School of Materials Science and Engineering, Shanghai Jiao Tong University, Shanghai, 200240, China

<sup>b</sup> Department of Chemical and Materials Engineering, The University of Auckland, Private Bag 92019, Auckland 1142, New Zealand

## ARTICLE INFO

### Article history:

Received 4 January 2011

Received in revised form 19 May 2011

Accepted 24 May 2011

Available online 6 June 2011

### Keywords:

Titanium alloys

Microstructure

Mechanical properties

Electrochemical characterization

Biomedical application

## ABSTRACT

We have fabricated a new  $\beta$  metastable titanium alloy that comprised of non-toxic elements Mo and Zr. Ingot with composition of Ti–12Mo–5Zr is prepared by melting pure metals in a vacuum non-consumable arc melting furnace. The alloy is then homogenized and solution treated under different temperature. The alloy is characterized by optical microscopy, X-ray diffraction, tensile tests and found to have an acicular martensitic  $\alpha'' + \beta$  structure and dominant  $\beta$  phase for the 1053 K and 1133 K solution treatment samples, respectively. The elastic modulus of the latter is about 64 GPa, which is much lower than those of pure Ti and Ti–6Al–4V alloy. In addition, it had moderate strength and much higher microhardness as compared with Ti–6Al–4V alloy. The results show better mechanical biocompatibility of this alloy, which will avoid stress shielding and thus prevent bone resorption in orthopedic implants applications. As long-term stability in biological environment is required, we have also evaluated the electrochemical behavior in a simulated body fluid (Hank's solution). Potentiodynamic polarization curves exhibits that the 1133 K solution treatment Ti–12Mo–5Zr sample has better corrosion properties than Ti–6Al–4V and is comparable to the pure titanium. The good corrosion resistance combined with better mechanical biocompatibility makes the Ti–12Mo–5Zr alloy suitable for use as orthopedic implants.

© 2011 Elsevier B.V. All rights reserved.

## 1. Introduction

Titanium-based alloys have become most attractive materials in biomedical applications due to their low density, excellent biocompatibility, better corrosion resistance and relatively good fatigue resistance [1,2]. So far the mainstream titanium biomaterials are pure titanium and Ti–6Al–4V alloy. Although commercial purity (c.p.) titanium offers better corrosion resistance and tissue tolerance, its relatively low strength and poor wear resistance restrict its usage to non-load-bearing applications such as pacemaker case and heart valve cages. The typical  $\alpha + \beta$  phase Ti–6Al–4V alloy, on the other hand, has achieved by far the greatest success in orthopedic implant applications because it has an excellent combination of strength and toughness along with good corrosion resistance. However, the concerns over the cytotoxicity of vanadium and aluminum on this alloy have been raised in the 1980s [3,4]. Vanadium could cause long-term health problems such as peripheral neuropathy and osteomalacia. Aluminum was reported to be a growth inhibitor of bone and possible induced Alzheimer's disease. In addition, a relatively high elasticity modulus mismatch between the

Ti–6Al–4V alloy (110 GPa) and the bone (3–20 GPa) induced stress shielding effect, which could cause insufficient loading on bone adjacent to the implant, leading to an eventual failure of the implant [5].

Therefore, it engines the development of non-toxic and low elastic modulus  $\beta$  or near- $\beta$  type titanium alloys for biomedical applications. Mo, Nb, Ta, Zr and Sn are selected as alloying elements to titanium because they are non-toxic and non-allergic [6] and also stabilize  $\beta$  phase showing lower elasticity modulus and greater strength. In recent years, Ti–Mo [7], Ti–Mo–Nb [8], Ti–12Mo–5Ta [9], Ti–13Nb–13Zr [10], Ti–35Nb–2Ta–3Zr [11], and Ti–29Nb–11Ta–5Zr [12] have been researched with emphasis on their microstructure, mechanical properties and corrosion resistance for medical applications. For example, Ti–13Nb–13Zr alloy in which Zr is used to replace Al was developed by Smith & Nephew Richards Inc. [13]. Two symbolic  $\beta$  alloys, Ti–12Mo–6Zr–2Fe and Ti–35Nb–7Zr–5Ta, showed an elastic modulus of 74–86 GPa and 55 GPa respectively and excellent biocompatibility [14,15].

In this paper, we discuss the microstructure and mechanical properties of a new TiMoZr alloy. The new Ti–12Mo–5Zr samples were characterized using optical microscope, XRD and tensile tests. The electrochemical behavior of this alloy was also investigated due to the corrosion behavior was of crucial interest for the biocompatibility in biomedical implants.

\* Corresponding author. Tel.: +86 21 34202759; fax: +86 21 34202759.  
E-mail address: [xnzhang@sjtu.edu.cn](mailto:xnzhang@sjtu.edu.cn) (X. Zhang).



Fig. 1. Microstructure of the Ti–12Mo–5Zr alloys: (a) homogenized; (b) 1053 K ST; and (c) 1133 K ST.

**Table 1**  
Chemical composition of the TiMoZr alloy.

Element	Mo	Zr	O	N	C	Fe	Ti
wt.%	12.05	5.3	0.08	0.01	0.012	0.038	Balance

## 2. Materials and methods

The TiMoZr alloy with a nominal composition (in weight fraction) of Ti–12Mo–5Zr was fabricated by vacuum non-consumable arc melting furnace. Due to the big difference in the melting point (Ti: 1943 K; Mo: 2890 K; Zr: 2125 K) and density (Ti: 4.5 g/cm<sup>3</sup>; Mo: 10.2 g/cm<sup>3</sup>; Zr: 6.49 g/cm<sup>3</sup>) of the pure metals, the ingot was re-melted three times to ensure compositional homogeneity. After that the alloy ingot was homogenized at 1273 K for 10 h in vacuum condition. Table 1 shows the chemical composition of the TiMoZr samples obtained by Varian's inductively coupled plasma optical emission spectrometer (ICP-OES).

The specimens were subjected to solution treatment (ST) at 1053 K and 1133 K for 1 h followed by a rapid water quenching. The microstructures observations of the as-homogenized, as-solution specimens were carried out by optical microscope. X-ray diffraction measurements were done at room temperature under the conditions of Cu K $\alpha$  radiation, 35 kV, and 200 mA (Rigaku, D/MAX255). Tensile tests were determined on MTS-810 system at a strain rate of  $1.5 \times 10^{-4}$  s at room temperature. Vickers hardness was measured using a HX-1000 hardness tester using a load of 200 gf and a dwell time of 15 s.

The corrosion behavior was investigated by electrochemical test on the CH Instruments 660D Electrochemistry Workstation in Hank's solution at 37 °C. Potentiodynamic polarization scans were carried out on the as-solution samples with a scan rate of 5 mV/s in the range from –1 V to 2 V vs. SCE. Commercial pure titanium (Grade 2) and Ti–6Al–4V were also tested for comparison. The chemical composition of Hank's solution includes: NaCl: 8 g/l, KCl: 0.4 g/l, CaCl<sub>2</sub>: 0.14 g/l, NaHCO<sub>3</sub>: 0.35 g/l, glucose: 1.0 g/l, MgCl<sub>2</sub>·6H<sub>2</sub>O: 0.1 g/l, MgSO<sub>4</sub>·7H<sub>2</sub>O: 0.06 g/l, KH<sub>2</sub>PO<sub>4</sub>: 0.06 g/l, Na<sub>2</sub>HPO<sub>4</sub>·12H<sub>2</sub>O: 0.06 g/l.

## 3. Results and discussion

Fig. 1 shows the microstructure of the homogenized and solution-treated specimens. The homogenized one shows a  $\alpha$ -phase microstructure seen from Fig. 1a. The 1053 K ST specimen (Fig. 1b), however, consists of a mixture of acicular martensitic  $\alpha''$  and  $\beta$  phase. The XRD patterns plotted in Fig. 2 confirmed the presence of these structures. The 1133 K ST specimen exhibits an equiaxed  $\beta$  phase microstructure with a grain size of a few tens of micrometers and no evidence of  $\alpha''$  precipitation in the beta matrix (Fig. 1c). Nevertheless, the X-ray diffraction profile in Fig. 2 shows the presence of martensite  $\alpha''$  phase. A possible reason is the precipitation of the orthorhombic martensite  $\alpha''$  phase cannot be detected with optical microscopy due to the small size.

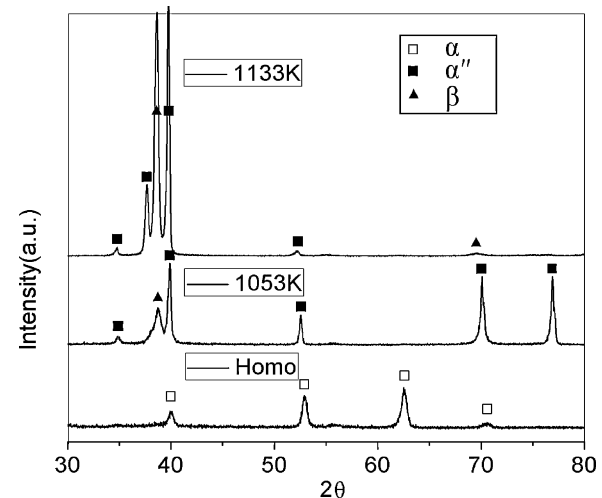


Fig. 2. XRD result of Ti–12Mo–5Zr with different heat treatment.

Molybdenum is a  $\beta$ -stabilizing element, whereas zirconium is usually regarded as a neutral element, which does not stabilise either  $\alpha$  or  $\beta$  phase. However, Zr addition does retard the martensitic transformation during cooling, thereby contributing to the hardenability [16]. Antipov and Moiseev [17] further commented that the addition of 6%Zr could produce an equivalent effect to that of 1.5%Mo. According to the coefficient of  $\beta$  stabilisation, the stability of  $\beta$  phase is quantified as:

$$K_{\beta} = \sum_i \frac{c_i}{\beta_{c,i}} \quad (1)$$

where  $c_i$  is the concentration of the  $\beta$ -stabilising element in the alloy and  $\beta_{c,i}$  is its critical concentration. The titanium alloys whose  $K_{\beta}$  are in the region of 1–1.5 (i.e.  $1 < K_{\beta} < 1.5$ ) was defined as metastable  $\beta$  alloys. For the Ti–12Mo–5Zr alloy, the  $K_{\beta}$  is 1.1, which classified this alloy in the metastable  $\beta$  category.

The mechanical characteristics of Ti–12Mo–5Zr alloy obtained by tensile and microhardness tests are summarized in Table 2. The Young's modulus of the TiMoZr alloy are much lower than that of the pure titanium and Ti–6Al–4V alloy reported in other literature [18], especially for the 1133 K solution treated Ti–12Mo–5Zr

**Table 2**  
Mechanical properties of the Ti–12Mo–5Zr alloy.

Alloys	Young's modulus (GPa)	Yield strength (MPa)	Ultimate tensile strength (MPa)	Elongation (%)	Hardness (HV)
Homogenized	90.9 ± 2.2	956 ± 23	1028 ± 16	4.1 ± 0.2	396 ± 13
1053 K ST	78.6 ± 1.7	540 ± 11	695 ± 25	3.9 ± 0.5	427 ± 20
1133 K ST	64.5 ± 0.3	509 ± 16	628 ± 32	4.7 ± 0.3	442 ± 8
c.p. Ti (grade 2) [18]	105	–	344	20	145
Ti–6Al–4V (grade 5) [18]	114	–	860	15	341

samples. It is known that Young's modulus is determined by the bonding force among atoms and greatly affected by the crystal structure. In their study of Ti–25at% Nb alloy, Yao et al. [19] calculated the Young's moduli of  $\alpha''$ ,  $\beta$  and  $\omega$  phase through Voigt–Reuss–Hill Approximation. They found that  $\beta$  phase had the lowest Young's modulus, which was 35.29 GPa compared to 46.93 GPa of  $\alpha''$  phase and 75.62 GPa of  $\omega$  phase. Other literatures [20,21] also reported that the  $\alpha$  phase has higher elastic modulus than the  $\alpha''$  phase, and the  $\beta$  phase has the lowest in the Ti alloys. In this paper, the 1053 K ST and 1133 K ST Ti–12Mo–5Zr alloy both possessed lower modulus due to the emergence of  $\alpha''$  and  $\beta$  phase, and with the  $\beta$  phase volume fraction increasing, the Young's modulus further decreased. Long-term experiments have shown that the high modulus titanium implants transfer insufficient load to adjacent remodeling bone and result in bone resorption and eventual loosening of the prosthetic devices [22]. The Young's modulus of 1133 K ST Ti–12Mo–5Zr is 64.5 GPa, which is much closer to natural bone, that will minimize the bone resorption arise from the stress shielding effect and consequently increase the long-term stability of the implants.

The yield strength and ultimate tensile strength of the TiMoZr alloy are much higher than that of pure titanium and comparable to that of Ti–6Al–4V alloy. The strength decrease in the solution treated samples is partly due to the dissolution of prior  $\alpha$  particles into  $\beta$  matrix, and partly due to  $\beta$  grain coarsening. As we know the strength of metals is strongly correlated to its microstructure, the finer microstructure processed by cold- or hot-work will greatly improve its tensile strength and elongation to failure. Another property, the permissible strain, is also important for orthopedic material design. The permissible strain is defined as the ratio of yield strength to ultimate strength, representing the deformation capacity of a mechanical construct. A good bio-metal should have a higher permissible strain than human cortical bone (0.67). In the homogenised state, the alloy Ti–12Mo–5Zr had a permissible strain of 0.93, while in the solution treated state, the permissible strain was 0.78 for 1053 K ST and 0.81 for 1133 K ST, which are comparable to that of Ti–6Al–4V and Ti–6Al–7Nb alloys [23]. It is known that the crystal structure/phase and grain size could affect the Vickers hardness of the alloys [8]. The 1133 K ST TiMoZr alloy with  $\beta + \alpha''$  phase had the highest Vickers hardness value (442 HV), while homogenized TiMoZr alloy with  $\alpha$  phase had the lowest hardness (394 HV). The Vickers hardness of 1053 K ST TiMoZr is slightly lower than that of 1133 K ST alloy, which is inconsistent with the tensile property results. That may be derived from the inhomogeneity of the samples.

Fig. 3 shows a representative potentiodynamic polarization curve for the Ti–12Mo–5Zr samples as compared with pure Ti

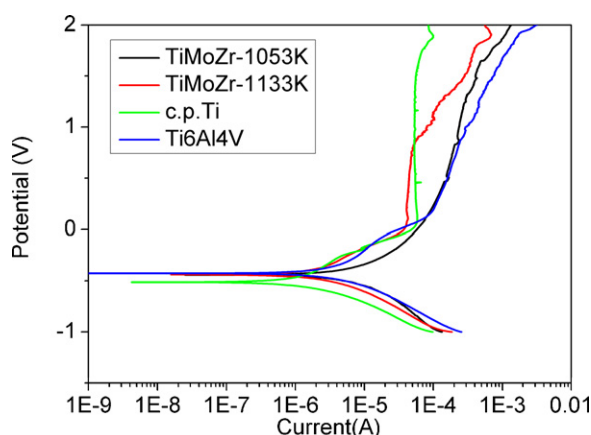


Fig. 3. Representative potentiodynamic polarization diagrams of TiMoZr samples after different heat treatment.

Table 3

Tafel analysis results obtained from polarization curves of Ti alloys in Hank's solution.

Alloys	$E_{\text{corr}}$ (V)	$i_{\text{corr}}$ ( $\mu\text{A}/\text{cm}^2$ )	$R_p$ ( $\Omega/\text{cm}^2$ )
1053 K ST	−0.682	−7.26	−11227
1133 K ST	−0.680	−3.70	−24781
c.p. Ti (grade 2)	−0.755	−0.62	−40108
Ti–6Al–4V	−0.668	−6.05	−16010

and Ti–6Al–4V in Hank's solution. The corrosion parameters determined from the Tafel region of the polarization curves are given in Table 3. Tafel analysis indicated that the corrosion potentials,  $E_{\text{corr}}$ , of the TiMoZr samples with different ST were similar. The corrosion current density,  $i_{\text{corr}}$ , of 1133 K ST Ti–12Mo–5Zr, however, was only half of the 1053 K ST sample and was also much lower than that of Ti–6Al–4V. The c.p. Ti possessed the lowest corrosion current density. The lower  $i_{\text{corr}}$  value of 1133 K ST sample suggested improvement in corrosion resistance property. The polarization resistance  $R_p$  determined from the linear polarization diagram listed in Table 3 showed that the  $R_p$  values decreased in sequence c.p. Ti > 1133 K ST > Ti–6Al–4V > 1053 K ST. The anodic branch of the polarization curve exhibited passive behavior associated with the protective films in 1133 K ST and c.p. Ti specimen. However, the 1053 K ST specimen and Ti–6Al–4V specimen did not show obvious passive regions.

The electrochemical results revealed that the corrosion resistance of the 1133 K ST Ti–12Mo–5Zr alloy is better than that of Ti–6Al–4V alloy and comparable to that of c.p. Ti. As Glass and Hong [24] had pointed out, the addition of Mo increased thermodynamic stability of titanium presumably due to its low diffusivity and promoted the resistance to pitting corrosion. Oliveira et al. [25] also showed that Ti–Mo alloys had good corrosion resistance in aerated Ringer solution. Another reason should be attributed to the changes occurred in the phases. As aforementioned and shown in Fig. 1, the 1053 K ST Ti–12Mo–5Zr is constituted by fine needle-like traces of  $\alpha''$  martensite. The 1133 K ST is consisted mainly of  $\beta$  phase. Min et al. [26] suggested that the  $\beta$  matrix with continuity and a high Mo content could maintain the stability of the passive film and showed high corrosion resistance against the crevice attack. As  $\alpha''$  phase (the less noble acicular phase) precipitating in the  $\beta$  phase (the nobler matrix phase), the galvanic corrosion effect [27] is inevitable and the corrosion resistance decreases. The good corrosion property combined with better modulus property and moderate strength and hardness, suggests the Ti–12Mo–5Zr alloy be an alternative material in orthopedic implant applications.

#### 4. Conclusion

In this work, a new near  $\beta$  type titanium alloy composed of non-toxic elements Mo and Zr has been developed. Based on the results obtained from this investigation on the microstructures, mechanical property and electrochemical corrosion, the following conclusions can be drawn. The new Ti–12Mo–5Zr alloy exhibits acicular martensitic  $\alpha'' + \beta$  structure and  $\beta$  phase after 1053 K and 1133 K solution treatment, respectively. The latter possesses a lower Young's modulus (about 64 GPa), moderate strength and higher microhardness which shows better mechanical biocompatibility in order to be used as orthopedic implants and to avoid stress shielding and thus prevent bone resorption and implant failure. The 1133 K ST Ti–12Mo–5Zr alloy also has a good resistance to corrosion in the electrochemical test as compared to Ti–6Al–4V. Thus, the new  $\beta$ -metastable Ti–12Mo–5Zr alloy can be an alternative biomaterial for orthopedic implant applications.

## Acknowledgements

The authors acknowledge the financial support for the work by the Nano Foundation of Science and Technology Commission of Shanghai Municipality (STCSM), China (Project no. 0852nm02800).

## References

- [1] H.J. Rack, J.I. Qazi, *Mater. Sci. Eng. C* 26 (2006) 1269–1277.
- [2] M. Long, H.J. Rack, *Biomaterials* 19 (1998) 1621–1639.
- [3] T. Rae., *J. Bone Joint Surg. Am.* 63B (1981) 435–440.
- [4] J.M. Candy, J. Klinowski, R.H. Perry, et al., *Lancet* 327 (1986) 354–357.
- [5] W.F. Ho, C.P. Ju, J.H. Chern Lin, *Biomaterials* 20 (1999) 2115–2122.
- [6] M. Niinomi, *Sci. Technol. Adv. Mater.* 4 (2003) 445–454.
- [7] N.T.C. Oliveira, A.C. Guastaldi, *Acta Biomater.* 5 (2009) 399–405.
- [8] L.J. Xu, Y.Y. Chen, Z.G. Liu, F.T. Kong, *J. Alloys Compd.* 453 (2008) 320–324.
- [9] D.M. Gordin, T. Gloriant, G. Nemtoi, et al., *Mater. Lett.* 59 (2005) 2936–2941.
- [10] V.S. Saji, H.C. Choe, *Corros. Sci.* 51 (2009) 1658–1663.
- [11] L. Wang, W. Lu, J. Qin, F. Zhang, D. Zhang, *J. Alloys Compd.* 469 (2009) 512–518.
- [12] P. Laheurte, F. Prima, A. Eberhardt, T. Gloriant, M. Wary, E. Patoor, *J. Mech. Behav. Biomed.* 3 (2010) 565–573.
- [13] S.B. Goodman, J.A. Davidson, V.L. Fornasier, A.K. Mishra, *J. Appl. Biomater.* 4 (1993) 331–339.
- [14] T. Ahmed, M. Long, J. Slivestri, C. Ruiz, H.J. Rack, in: P.A. Blenkinsop, W.J. Evans, H.M. Flower (Eds.), *Titanium'95: Science and Technology*, Institute of Metals, London, 1996, pp. 1760–1767.
- [15] K. Wang, *Mater. Sci. Eng. A* 213 (1996) 134–137.
- [16] E.W. Collings, in: W. Soboyejo, T.S. Srivatsan (Eds.), *Advanced Structural Materials*, ASM, Metals Park, OH, 1984, p. 261.
- [17] A.I. Antipov, V.N. Moiseev, *Met. Sci. Heat Treat.* 39 (1997) 499–503.
- [18] E. Bertrand, T. Gloriant, D.M. Gordin, E. Vasilescu, P. Drob, C. Vasilescu, S.I. Drob, *J. Mech. Behav. Biomed.* 3 (2010) 559–564.
- [19] Q. Yao, H. Xing, W.Y. Guo, J. Sun, *Rare Met. Mater. Eng.* 38 (2009) 663–666.
- [20] Y.L. Zhou, M. Niinomi, *J. Alloys Compd.* 466 (2008) 535–542.
- [21] Y.L. Zhou, M. Niinomi, T. Akahori, *Mater. Sci. Eng. A* 371 (2004) 283–290.
- [22] M. Geetha, K.U. Mudalki, A.K. Gogia, R. Asokamani, B. Raj, *Corros. Sci.* 46 (2004) 877–892.
- [23] S.G. Steinemann, *Periodontology* 2000 (17) (1998) 7–21.
- [24] R.S. Glass, Y.K. Hong, *Electrochim. Acta* 29 (1984) 1465–1470.
- [25] N.T.C. Oliveira, G. Aleixo, R. Caram, A.C. Guastaldi, *Mater. Sci. Eng. A* 452–453 (2007) 727–731.
- [26] X.H. Min, S. Emura, T. Nishimura, et al., *Mater. Sci. Eng. A* 527 (2010) 1480–1488.
- [27] A. Cremasco, W.R. Osório, C.M.A. Freire, A. Garcia, R. Caram, *Electrochim. Acta* 53 (2008) 4867–4874.